# Neeaj Yadav

## Alakli-Modified Kalanchoe Pinnata Leaves As A Biosorbent For Sequestration Of Crystal Violet Dye.docx

MTech report

MTech2025

India Institute of Technology Delhi

### Document Details

Submission ID
trn:oid:::1:3602918833

Submission Date
Jun 28, 2026, 8:08 PM GMT+5:30

Download Date
Jun 28, 2026, 8:12 PM GMT+5:30

File Name
Alakli-Modified_Kalanchoe_Pinnata_Leaves_As_A_Biosorbent_For_Sequestration_Of_Crystal_Viol....docx

File Size
8.7 MB

36 Pages

7,894 Words

45,959 Characters

# 1% Overall Similarity

The combined total of all matches, including overlapping sources, for each database.

## Filtered from the Report

- Bibliography
- Quoted Text
- Small Matches (less than 14 words)

## Exclusions

- 1 Excluded Source

## Match Groups

**5** Not Cited or Quoted 1%
Matches with neither in-text citation nor quotation marks

**0** Missing Quotations 0%
Matches that are still very similar to source material

**0** Missing Citation 0%
Matches that have quotation marks, but no in-text citation

**0** Cited and Quoted 0%
Matches with in-text citation present, but no quotation marks

## Top Sources

0% Internet sources
1% Publications
1% Submitted works (Student Papers)

## Match Groups

- **5** Not Cited or Quoted 1%
  Matches with neither in-text citation nor quotation marks
- **0** Missing Quotations 0%
  Matches that are still very similar to source material
- **0** Missing Citation 0%
  Matches that have quotation marks, but no in-text citation
- **0** Cited and Quoted 0%
  Matches with in-text citation present, but no quotation marks

## Top Sources

0% Internet sources
1% Publications
1% Submitted works (Student Papers)

## Top Sources

The sources with the highest number of matches within the submission. Overlapping sources will not be displayed.

1 Student papers
**Delhi Technological University** <1%

2 Publication
**Shihua Zheng, Dong Shen, Kangdi Chen, Jiuhong Wei, Guoqiang Li, Guojie Zhang. ...** <1%

3 Publication
**Tra Huong Do, Thị Nguyet Hua, Manh Nhuong Chu, Thi Hien Lan Nguyen, Truong ...** <1%

# Chapter 1
# INTRODUCTION & LITERATURE REVIEW

In recent decades, industrialization, urbanization, and agricultural practices have increased the introduction of pollutants into aquatic ecosystems, including heavy metals, synthetic dyes, pharmaceutical residues, pesticides, and organic compounds [1]. Therefore, in this century, one of the most pressing environmental issues is water pollution [2]. As a result, aquatic life, ecosystem stability, and human health have been adversely affected by persistent and toxic pollutants. Among existing effluents, cationic dyes such as crystal violet are among the most hazardous to aquatic life and other living beings in nature due to their widespread use across industries, including ink printing, textiles, paper, and dyeing. It also has extremely harmful effect on ingestion and can result in cyanosis, irritated skin, irreversible blindness, itchy eyes, dizziness, staining of skin, and elevated heart rate [3], [4]. Therefore, to protect life, it must be eliminated before industrial wastewater is released into water sources. Traditionally, technologies such as chemical precipitation, filtration, chemical coagulation, activated carbon, and ion exchange methodology have been adopted to address this issue[5], [6], [7]. However, these approaches are expensive and less effective, with limitations such as being unsustainable, toxic, non-reproducible, difficult to operate, and requiring toxic precursors[8]. Hence, the use of biomass-derived materials as adsorbents for removing pollutants from aqueous environments has become increasingly popular among researchers due to their eco-friendly, cost-effective, ease of synthesis, and sustainable characteristics [9], [10]. This growing emphasis on preserving pollutant-free water bodies has given rise to the concept of ‘Bio-based adsorption. Biosorption is a cost-effective and economically viable approach for the sequestration of pollutants [11], [12], [13]. The biosorbents are rich in bioactive compounds

that contain multiple functional groups capable of forming complexes or binding with metal ions, dyes, and organic pollutants [12], [13], [14].

According to studies, significant amounts of biowaste are generated annually, including seeds, fruit peels, stems, leaves, flowers, shells, biomass, stalks, and grasses. The use of these low-value materials as biosorbents can yield significant environmental benefits in controlling pollution and waste management [15], [16], [17], [18]. Plant-based biosorbents are gaining attention nowadays due to their key characteristics, which include biodegradability, renewability, non-toxicity, abundance, and easy accessibility in large quantities as agricultural waste. The Leaf-based biosorbents exhibit high efficacy in dye removal due to their unique composition, which encompasses cellulose, polyphenols, hemicelluloses, pectin, and lignin [19], [20]. As a result, numerous researchers have studied green biosorbents made from several biowaste, including orange peel, water chestnut peel, brinjal, cadamba waste pulp, and biochar [17], [20], [21], [22], [23], [24].

Among various plant-derived materials, "*Kalanchoe pinnata*", a plant belonging to the *Crassulaceae* family, has attracted scientific attention due to its diverse physicochemical properties [25]. This plant is widely available in tropical and subtropical regions and is known by several common names, such as '*Patharchatta*' in India. It has thick, fleshy leaves with a high-water content [26] . Historically, *Kalanchoe pinnata* has been valued in traditional medicine systems for its wound-healing, anti-inflammatory, anti-microbial, and diuretic properties [27]. However, recent scientific investigations have highlighted the potential of dried leaves in 'environmental remediation', especially in the 'adsorptive removal of pollutants' from contaminated water sources [28]. It contains flavonoids, phenolic acids, and triterpenoids, having polar functional groups-such as hydroxyl (-OH), carboxyl (-COOH), and carbonyl (-C=O) – onto the biomass surface. These functional groups are chemically reactive and assist the interaction between cationic dyes, heavy metals, and other organic molecules

[29]. It may lead to an effective and economically viable solution, which also aligns with the global vision of green chemistry and the principles of a circular economy [30]. Therefore, using leaves to remove contaminants is a cost-effective solution for water treatment and also supports resource recovery since discarded leaves can be reused for adsorption. Thereby, utilizing its leaves for pollutant removal not only provides a low-cost treatment option but also contributes to waste valorization, as discarded or naturally shed leaves can be employed for adsorption without harming the plant.

Among the various pollutants, cationic dyes are more toxic and pose a threat to both aquatic and human life [31], [32]. The dye Crystal Violet (CV) is a triphenylmethylamine with a molecular formula of $C_{25}H_{30}N_3Cl$. It induces genetic damage and cellular toxicity, making it a genotoxic and mitotoxic agent and classified as a recalcitrant dye molecule because it is chemically stable, resistant to degradation, and persists in the environment for extended periods[33], [34]. It causes skin irritation, redness, permanent skin discoloration, allergic reactions, dermatitis, and tissue necrosis [33]. Therefore, Crystal Violet is considered a significant biohazard to the ecosystem [8], [35].

*Kalanchoe pinnata* (KP), commonly known as 'Pathhar Chatta', is an indigenous plant with leaves that have not been alkali-activated yet, and have not been utilized for the sequestration of crystal violet dye from aqueous medium through the batch adsorption method.

In accordance with the literature, there are no prior reports for alkali-activated KP waste for the sequestration of cationic Crystal Violet (CV) dye**.** The NaOH-activated KP leaves demonstrated an impressive adsorption. The fabricated biosorbent has a higher active surface area than the non-activated KP leaves. The biomass-based sorbent offers an effective approach and introduces a novel, eco-friendly, green, facile, and scalable alternative to conventional, expensive adsorbents, highlighting its potential for real-world wastewater treatment applications.

The present study focuses on the synthesis of KP leaves-based biosorbent for the effective adsorption of CV dye from water. The KP was modified with sodium hydroxide (NaOH) and used to remove the crystal violet dye by the batch method. Alkali activation helps reduce lignocellulosic content in the adsorbent, making it more sustainable and water-stable. This study systematically investigates the effects of several physicochemical parameters on the adsorption of the synthesized biosorbent.

# Chapter 2
# MATERIALS AND METHODS

## 2.1 Materials

*Kalanchoe pinnata* (pathharchatta) plant leaves were collected from the Rewari district of Haryana, India. Crystal Violet (CV) dye were procured from ThermoFisher Scientific. Sodium hydroxide (NaOH), ethanol, and acetone were obtained from SRL Chemicals, Delhi, India, while hydrochloric acid (HCl) and acetone were purchased from CDH, India. All experiments were carried out using distilled water throughout the study.

## 2.2 Instruments

Fourier Transform Infrared (FTIR) spectra were recorded to identify functional groups present on the adsorbent surface using a PerkinElmer FTIR spectrometer in the range of 400–4000 $cm^{-1}$. Powder X-ray Diffraction (PXRD) patterns were employed to determine the crystallinity of the structure obtained using a Bruker D8 Advance X-ray diffractometer with $\lambda = 1.5418$ Å over a $2\theta$ range of 5–80°. A Field Emission Scanning Electron Microscopy (FESEM) microscope was used to study surface morphology using a JEOL JSM-6610LV. The BET–BJH methods were used to check the specific surface area and pore size distribution. The BET surface area was measured from $N_2$ adsorption–desorption isotherms at 77 K using a Quantachrome NovaWin. The biomass was degassed at 75 °C for 2 h under inert gas. The zeta potential of the nanoparticles was measured by Dynamic Light Scattering (DLS) using a Malvern Zetasizer Nano-ZSP. UV–Visible absorption spectra were recorded with a Shimadzu UV–Vis 1900i spectrophotometer at $\lambda\_max = 591$ nm. The pH of the solution was adjusted and maintained using an Eutech Scientific Thermo Fisher pH meter. To ensure reproducibility and reliability of the results, every study was performed in triplicate.

# Chapter 3
# EXPERIMENTAL SECTION

## 3.1 Synthesis

### 3.1.1 Collection and Preparation of Activated Kalanchoe Pinnata (AKP)

KP leaves were collected from Rewari, Haryana, in October 2024. The leaves were washed with tap water, then with distilled water, to remove surface dirt. Then, the leaves were placed in sunlight to remove moisture on their outer surfaces and subsequently heated in an oven at 60 °C to ensure complete dehydration. The dried leaves were then ground with a mortar and pestle. The resulting powder was then sieved to obtain a fine, uniform powder. Finally, the powdered leaves were stored in an airtight container for further study.

For the activation, 2 g KP leaves powder was suspended in 100 mL of 1 M NaOH solution and stirred for 4 hours. After that, the mixture was filtered, and the solid residue was thoroughly washed with distilled water until the pH was neutral. Then, the activated KP was dried at ambient temperature to obtain the desired dried activated adsorbent, which was further used in the sequestration of crystal violet dye from an aqueous solution. The choice of 1 M NaOH was based on its demonstrated effectiveness in modifying lignocellulosic materials by enhancing surface properties conducive to adsorption. Alkaline treatment with NaOH helps remove surface impurities, partially disrupt lignin and hemicellulose, and increases exposure of functional groups such as hydroxyl and carboxyl groups, thereby improving adsorption site accessibility and adsorbate interaction. The 1 M concentration is widely reported in the literature as an optimal balance, providing effective activation without causing significant structural degradation. Additionally, the biosorbent was thoroughly washed with distilled water until neutral pH was reached to eliminate residual NaOH and ensure environmental safety. Dey and his group have reported a similar methodology for activation [36], [37]. Although NaOH activation is effective to enhance adsorption properties, but it may raise environmental

concerns due to the generation of alkaline waste. Therefore, to avoid it, proper neutralization was done to minimize potential environmental impacts before discharge.

**Figure. A:** Kalanchoe Pinnata Leaves

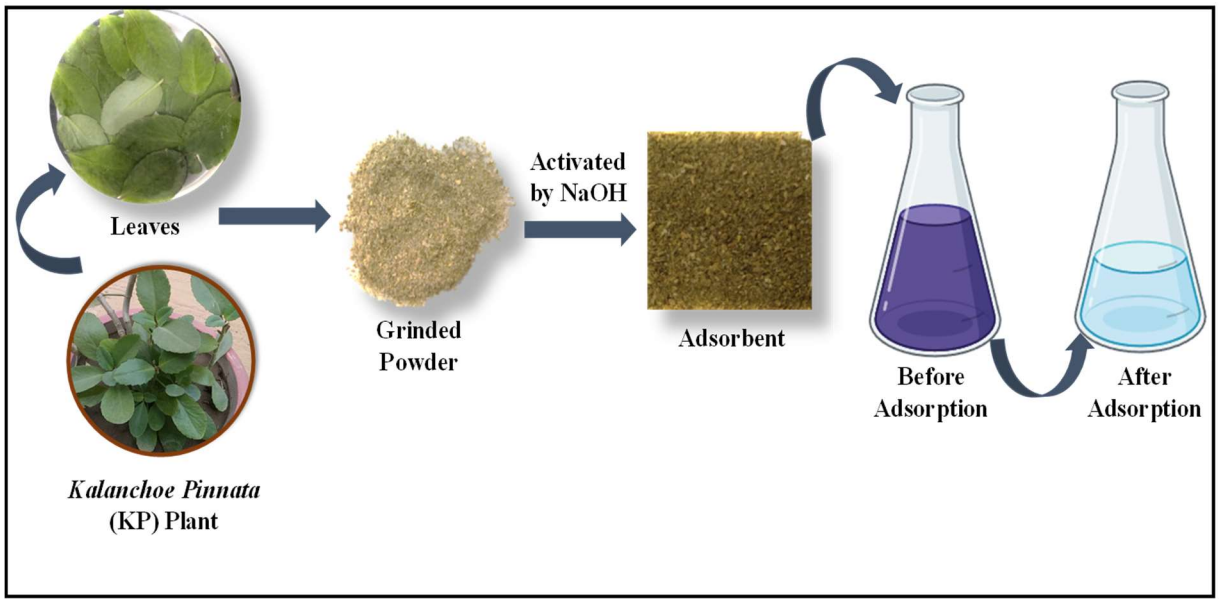


**Figure. B:** Schematic Representation of the activation of KP Leaves

## 3.2 Batch Analysis

To evaluate the adsorption efficiency, batch adsorption experiments of alkali-activated KP were conducted at 35 °C. For the adsorption study, 0.15 g of AKP was added to 0.1 L of crystal violet (CV) solution with an initial concentration of 30 mg $L^{-1}$. The mixture was agitated in the dark for 90 min. The pH of the solution was adjusted with 1 M NaOH and 1 N HCl. Then, 3 mL aliquots were collected at 10-minute intervals, and the collected aliquots were used to determine the CV concentration using a Shimadzu UV–Vis spectrophotometer at $\lambda_{max}$ = 591

nm. Similarly, studies were performed, including a pH study (3.5-9.5), adsorbent dosage (0.05-0.25g), dye concentration (20-80 mg/L), initial dye concentration (30 mg/L), and the effect of temperature (25-45 °C). To calculate maximum equilibrium adsorption capacity ($q_e$), and adsorption percentages (% R), using equations (1) and (2) [24], [38]:

$$\% R = \frac{C_0 - C_t}{C_0} \times 100 \quad (1)$$

$$q_e = (C_0 - C_t) \times \left(\frac{V}{W}\right) \quad (2)$$

Here, $C_0$, $C_t$, and $C_{eq}$ represent the initial, final, and equilibrium concentrations of the CV dye solutions.

## 3.3 Point Zero Charge

Point zero charge ($pH_{PZC}$ ) is a point where the surface of a material turns neutral. The surface shows a positive charge when its pH is below $pH_{PZC}$ and a negative charge when it is higher than $pH_{PZC}$. The experiment includes an electrolytic aqueous solution range from pH 2 to 11. After adjusting the pH of the solution, 0.025 g adsorbent was added to the individual pH's solution and then kept stable for 24 h. Then, the final pH was measured, a plot was made between ΔpH vs pH, and the point where the plotted line intersects the $x$ -axis refers to $pH_{zc}$ [39].

## 3.4 Isotherms

The interaction between the dye molecules and the adsorbent surface was analyzed using adsorption isotherm models, which describe the relationship between the amount of dye adsorbed and its equilibrium concentration in solution.

The Langmuir isotherm assumes monolayer adsorption of dye molecules onto a homogeneous surface with uniform adsorption sites, where intermolecular interactions between adsorbed species are negligible. Each adsorption site is considered energetically equivalent and

independent, with no mutual influence among neighboring sites. The linearized form of the Langmuir isotherm equation is expressed in Equation (3) [40]. The linear equation for the Langmuir model is

$$\frac{c_e}{q_e} = \frac{1}{k_L q_{max}} + \frac{c_e}{q_{max}} \qquad (3)$$

where $q_{max}$ (mg/g) and $q_e$ (mg/g) represent the maximum adsorption capabilities and the equilibrium adsorption capacities of CV, respectively. While equilibrium concentrations of CV are represented by $C_e$ (mg/L) and the Langmuir constant is represented by $K_L$ (L/mg).

$R_L$ is a dimensionless constant that is used to determine linearity (RL=1), irreversibility (RL=0), favourability (0 < RL <1), or unfavourability ($R_L$ > 1) of adsorption and is calculated with the given formula.

$$R_L = \frac{1}{1+k_L C_0} \qquad (4)$$

Where CV solution concentration (mg/L) is given by $C_0$.

The Freundlich isotherm describes adsorption on a heterogeneous surface with sites of varying affinities and energies. It assumes a multilayer adsorption process in which the amount of dye adsorbed increases with equilibrium concentration but at a decreasing rate. This empirical model is particularly suitable for non-ideal adsorption on heterogeneous surfaces.

The linearized form of the model is expressed as [41].

$$\log q_e = \log K_f + \frac{1}{n_f} \log C_e \qquad (5)$$

Here, $q_e$ refers to adsorption capacities (mg $g^{-1}$), and Ce represents the equilibrium concentration of CV dye (mg $L^{-1}$). While Freundlich coefficients, $K_f$ [(mg $g^{-1}$) (L $mg^{-1}$) $^{1/n_f}$], represent the adsorption capacity of the adsorbate, and nf indicates the heterogeneous adsorption intensity.

The Temkin isotherm accounts for interactions between the adsorbate and the adsorbent

surface, assuming that the heat of adsorption decreases linearly with increasing surface coverage. This model suggests that adsorption occurs through a uniform distribution of binding energies up to some maximum binding energy [42].

$$q_e = \frac{RT}{b} \ln A + \left(\frac{RT}{b}\right) \ln C_e \qquad (6)$$

RT/b = $B_T$, where R is the gas constant (8.314 J mol/K), T is the absolute temperature in Kelvin (K), and B represents the heat of adsorption (J/mol).

## 3.5 Kinetics

The adsorption kinetics and adsorption interaction mechanism between the adsorbent and adsorbate were examined using the pseudo-first-order, pseudo-second-order, and Elovich kinetic models [43], [44]

The pseudo-first-order model assumes that the adsorption rate is governed by the number of unoccupied active sites on the adsorbent surface, which can be represented as a linear equation

$$\ln(q_e - q_t) = \ln q_e - K_1 t \qquad (7)$$

Here, $q_e$ is the adsorbent uptake capacity (mg/g) of dye at equilibrium and and $q_t$ is uptake capacity at time 't.' $K_1$ is rate constant ($min^{-1}$).

The pseudo-second-order kinetic model assumes that the rate of adsorption is proportional to the square of the number of unoccupied sites, and its linearized form is expressed as [45]:

$$\frac{t}{q_t} = \frac{1}{k_2 q_e^2} + \frac{t}{q_e} \qquad (8)$$

Here, $q_e$ represent the dye uptake of adsorbent at equilibrium and $q_t$ (mg/g) represent uptake at the time 't'. The rate constant is determined by $k_2$ ($min^{-1}$).

The initial adsorption rate 'h' (mg/g/$min^1$) can be determined by the equation

$$h = k_2 q_e^2 \qquad (9)$$

According to the Elovich model, the adsorption process occurs on a heterogeneous surface where the activation energy for chemisorption varies exponentially with surface coverage. The model is expressed in its linear form as [46]:

$$q_t = \frac{1}{\beta}\ln(\alpha\beta) + \frac{1}{\beta}\ln t \qquad (10)$$

$q_t$ (mg/g) shows the uptake capacity of dye at the time 't,', β is the desorption constant (g/mg), and α is the initial rate of adsorption (mg/g/min).

# Chapter 4
# RESULT AND DISCUSSION

## 4.1 CHARACTERISATION

### 4.1.1 Functional Group Analysis (FTIR)

The FTIR spectra of KP and activated KP are shown in Figure 1, which reveal the functional groups present in the materials. It was observed that no significant difference was observed in the FTIR spectra of KP and activated KP [47]. In KP, the broadband at 3339 $cm^{-1}$ is attributed to the OH band, which may be associated with cellulose and lignin. The peaks at 2915 $cm^{-1}$ and 2852 $cm^{-1}$ are associated with the asymmetric C–H vibrations of alkyl groups. The bands at 1726 $cm^{-1}$ and 1634 $cm^{-1}$ confirm the presence of C=O and C=C aromatic groups in hemicellulose and lignin. The peak at 1023 $cm^{-1}$ is associated with C–H bonds in cellulose. While, in case of activated KP, intensity of the peak associated with OH band increased due to dehydration and reduction of the hydroxyl group after activation, and it was found to be at 3299 $cm^{-1}$ [48]. The intensity associated with asymmetric C-H stretch was found to be less in KP, which may be attributed to the activation of the material [49]. The peak at 1604 $cm^{-1}$ intensifies and may be attributed to partial oxidation, indicating a modification of the carbonyl group [50]. While less prominent band was observed at 1023 $cm^{-1}$ present in activated KP may be attributed to the disruption of polysaccharide structure, which may lead to enhancement of carbon content, resulting in higher surface area and thereby enhanced adsorption in activated KP [51], [52].

Additionally, FTIR analysis was also performed after adsorption. It was observed that almost similar analysis was observed after adsorption. The only difference is decrement in peak position and there is a slight shift in peak position may suggests that there is some interaction taking place with the material [42]

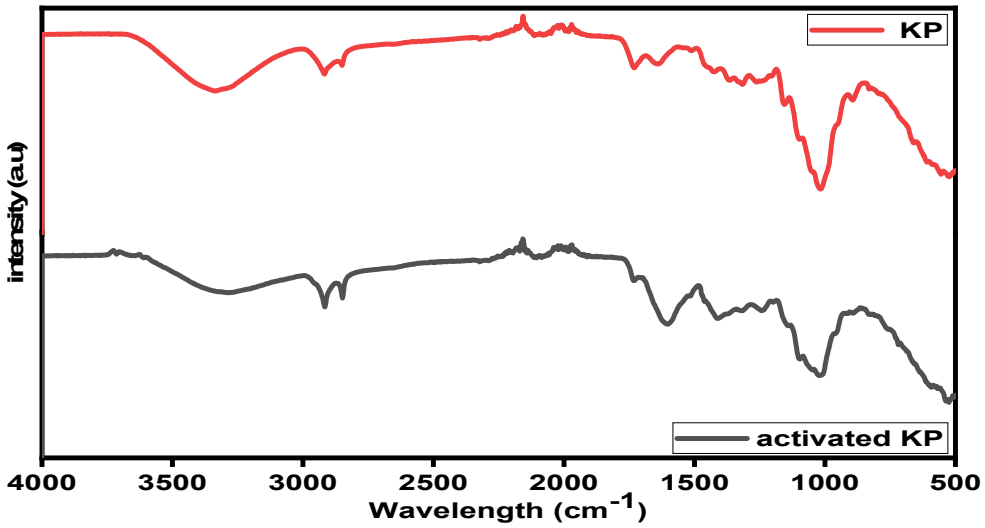


**Figure 1.** FTIR spectra for the KP and activated KP.

### 4.1.2 Crystallinity Analysis (XRD)

The XRD pattern of KP and activated KP is presented in Figure 2. The XRD pattern of KP exhibits a prominent peak at 21°, which may be attributed to the semi-crystallinity present in the material due to cellulose. The minor sharp peaks at 28.33° and 40° in KP are attributed to the presence of residual inorganic components present in KP [53]. While a more pronounced broad band in activated KP was found at 21.44°, and a prominent peak at 29.49°, suggesting enhanced crystalline characteristics in the activated KP, minor peaks from 35-46° in activated KP indicated that the chemical activation of KP leads to a crystalline nature, thereby reducing hemicellulose and cellulose content [54]. Hence, it may be inferred that the breakdown of cellulose and lignin due to activation, which may further lead to enhancing the active surface area [51], [55].

Moreover, to check the structural integrity, XRD analysis was performed after adsorption. It was observed that there is no shift or disappearance of peak was observed in adsorbent after adsorption, but decrement in intensity was observed that may be due to regeneration cycles for adsorption.

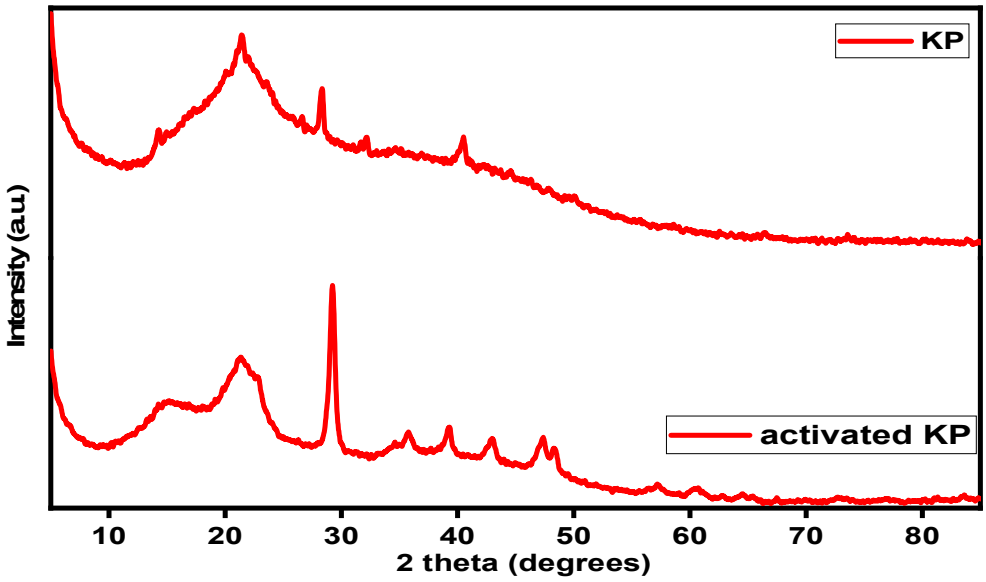


**Figure 2.** The plot of XRD for KP and activated KP

### 4.1.3 Morphology Analysis (FESEM)

The micrographs of KP and activated KP are presented in Figure 3. In KP, smooth and layered structures with irregular particles were obtained, whereas in activated KP, rough surfaces, more porous, and fragmented morphologies were observed [56]. This may lead to an enhancement in adsorption capacity due to the increased availability of adsorption sites, resulting in comparatively enhanced adsorption in activated KP.

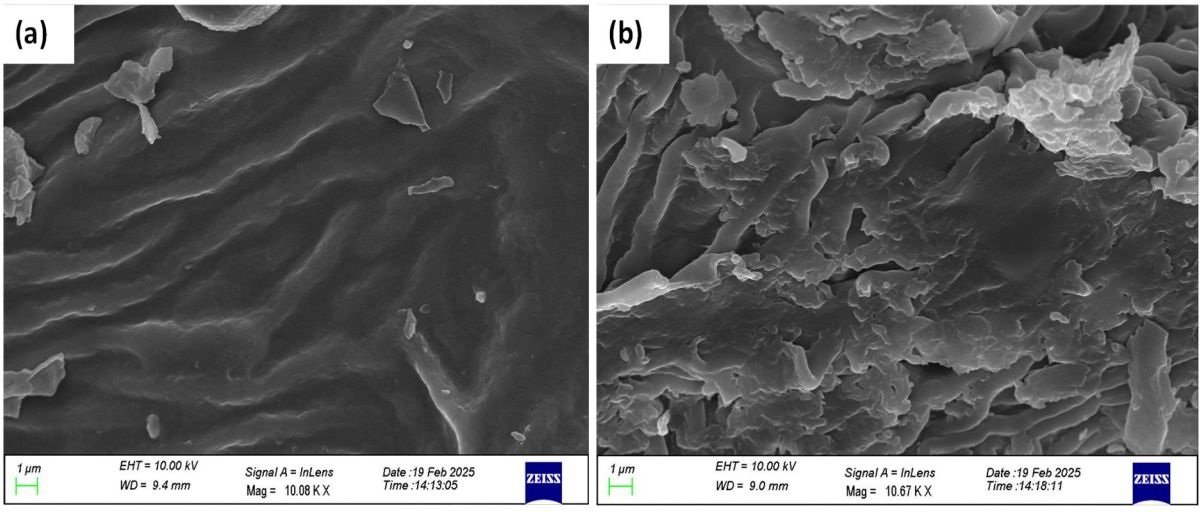


**Figure 3.** FESEM images of (a) KP and (b) Activated KP.

### 4.1.4 Surface Charge Analysis (DLS)

This method is used to determine the zeta potential of the synthesized biosorbent, as shown in Figure 4. It will provide information on the stability and charge of the biosorbent. In KP, a slightly negative charge was obtained, which may lead to less electrostatic interaction. In contrast, activated KP exhibited an increase in negative surface charge, resulting in a greater electrostatic interaction and, consequently, a more pronounced adsorption of dye molecules over the biosorbent surface [12]. It may be concluded that activated KP has higher negative charge, suggesting that the stronger electrostatic interaction between adsorbent to the adsorbate, leads to greater removal of CV from aqueous media. While lesser negative charge leads to lesser electrostatic interaction, attributed to lesser removal of CV using KP.

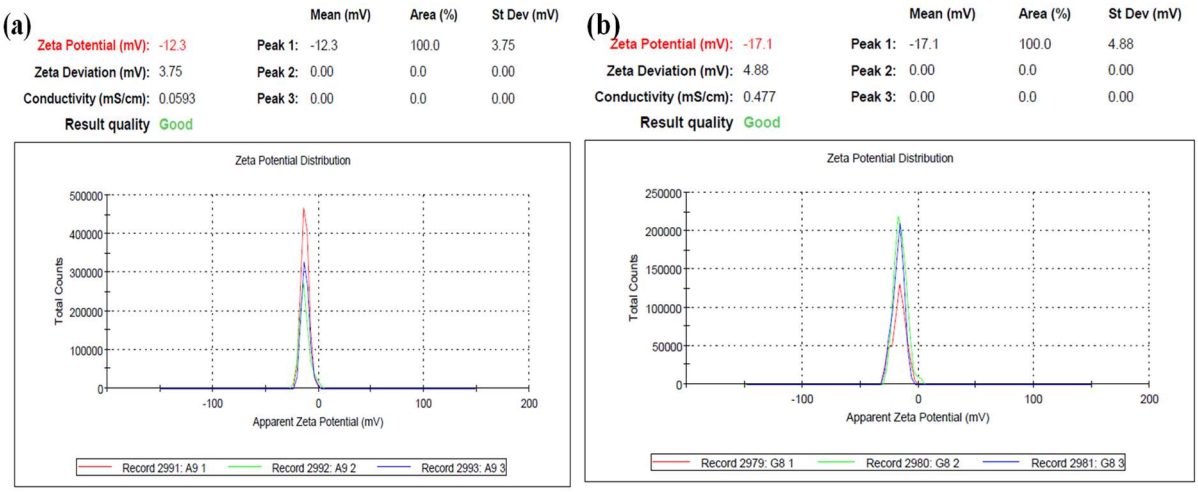


**Figure 4.** The plot for the Zeta potential of (a) KP and (b) activated KP

### 4.1.5 Surface Area Analysis (BET)

The surface areas of KP and AKP were estimated using the Brunauer-Emmett-Teller (BET) method and found to be 5.719 $m^2/g$ and 12.097 $m^2/g$, respectively. The plot for activated KP is presented in Figure 5. The pore volumes for KP and activated KP were measured using the BJH method and were found to be 0.003 cc/g and 0.004 cc/g, respectively. The pore radius was found to be 16.124 Å and 19.279 Å, respectively. It was observed that a Type I isotherm for activated KP was present, indicating that the material exhibits both mesoporous and

microporous characteristics [8], [57]. Therefore, it is concluded that upon alkali activation, the surface area of KP increases, allowing for enhanced adsorption in activated KP.

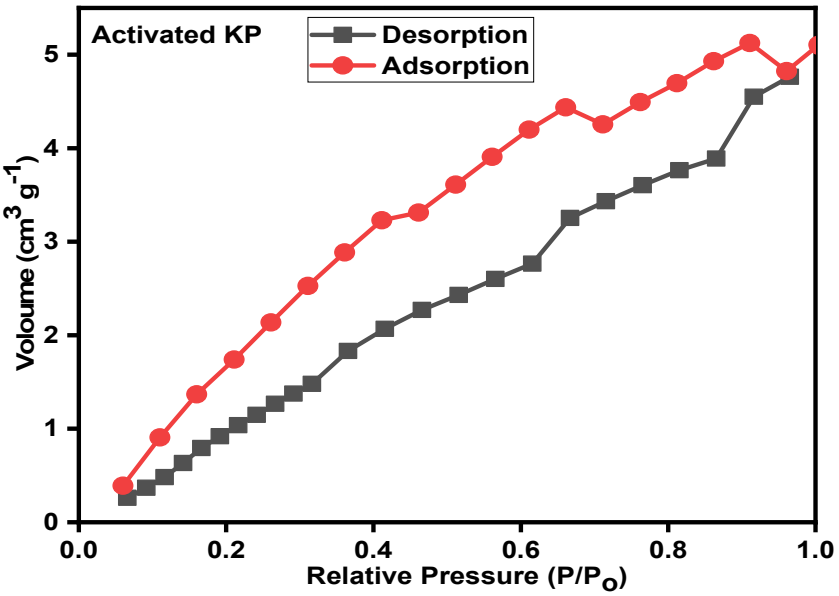


**Figure 5.** $N_2$ adsorption-desorption BET analysis of activated KP

## 4.2 Adsorption Studies

### 4.2.1 Impact of Equilibrium Time

The adsorption efficiency is strongly influenced by the contact time between the adsorbent and the dye solution, as this determines the adsorption equilibrium time. The percentage removal of crystal violet (CV) dye by alkali-activated KP is presented in Figure 6. At the beginning of the adsorption process, 60% dye removal was achieved within 15 minutes, gradually increasing to 88% in 60 minutes and to 96% in 90 minutes, as shown in **Figure 6**. There was no significant difference in adsorption efficiency beyond this point, indicating saturation in the adsorbent. It may imply that during the initial phase, a high number of active sites were available on the surface of activated KP, resulting in rapid adsorption [51]. The number of vacant sites decreased as contact time increased, leading to equilibrium in the adsorption process. Similarly, the adsorption study was conducted without activated KP, and the dye adsorption was 69%. Therefore, a further study was conducted on activated KP. Hence, the contact time for the further studies is 90 minutes [35].

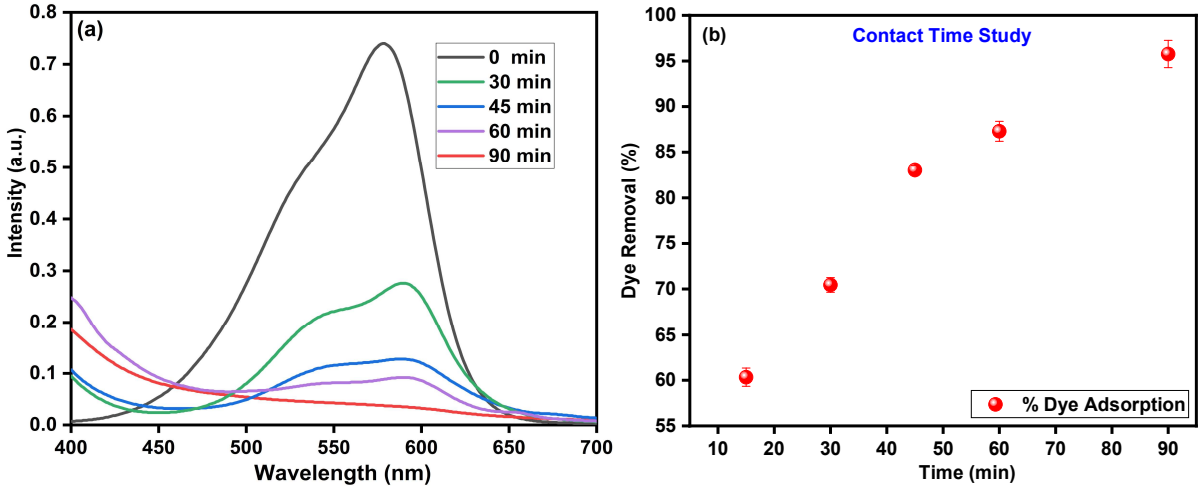


**Figure 6.** (a) UV-visible adsorption spectra, (b) Contact time vs dye adsorption (%) using activated KP.

### 4.2.2 Impact of Dye Concentration

The impact of concentration on adsorption efficiency was evaluated in the range of 20-80 mg/L, as illustrated in Figure 7a. The results reveal that as the dye concentration increased, the percentage removal of CV decreased from 96% to 50% at 50 mg/L. This trend can be explained by the limited availability of active sites on the adsorbent surface. As the dye concentration increases, the number of CV molecules in solution exceeds the available adsorption sites, leading to saturation of the active surface and a decrease in adsorption efficiency [58], [59].

### 4.2.3 Impact of Adsorbent Dosage

The influence of adsorbent dosage on the removal efficiency of the CV dye was investigated to identify the optimal adsorbent dosage. For this study, varying doses of adsorbent (0.05-0.25g) were studied with a 30 mg/L CV dye solution, as illustrated in Figure 7b. The results revealed that the percentage of dye removal increased from 77% to 97% as the adsorbent dosage varied from 0.05 g to 0.25g. This enhancement in adsorption efficiency can be attributed to the availability of active sites in the starting state and to the increased surface area of the adsorbent, which facilitate more interactions between the dye and the adsorbent [60]. However, no increment in dye removal was observed on further increasing the adsorbent

(0.2g). It may be due to the overlapping or aggregation of adsorbent particles at higher dosages, which reduces the effective surface area and consequently decreases the number of accessible active sites for adsorption [61]. Additionally, the excessive adsorbent mass may cause a reduction in dye concentration per unit mass of adsorbent, resulting in incomplete utilization of available sites. Thereby, the higher the amount of adsorbent, the less the interaction of the dye molecule onto the adsorbent surface. Therefore, an optimal adsorbent dosage of 0.15 g was determined to achieve maximum adsorption efficiency.

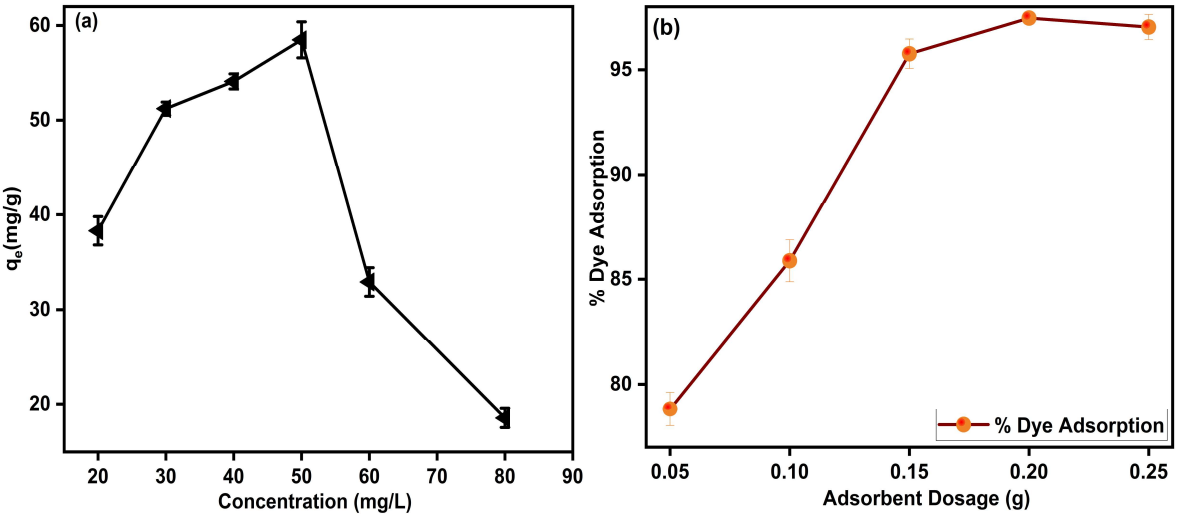


**Figure 7.** Plots of (a) Impact of dye concentration and (b) Impact of adsorbent dosage.

### 4.2.4 Impact of pH

The pH of the solution plays a significant role in altering the surface charge density of the adsorbent and controlling interactions between the adsorbent and the adsorbate. The impact of pH on CV adsorption by activated KP was monitored in the pH range of 3.5-9.5, using 0.15g of adsorbent and a 90-minute reaction time, as presented in Figure 8a. It was observed that the percentage of dye adsorption increased from 78% to 96% as the pH was increased from 3.5 to 8.5. An increase in pH from 8.5 resulted in a decrease in % dye adsorption. This can be correlated with the ($pH_{ZPC}$) zero-point charge, which was found to be 7.94. The $pH_{ZPC}$ value determines the surface charge of the adsorbent in relation to the solution's pH, presented in Figure 8b. When the pH of the solution is less than $pH_{ZPC}$, the adsorbent surface acquires a

positive charge; at pH values greater than $pH_{ZPC}$, the surface becomes negatively charged. Because, at lower pH ($pH < pH_{ZPC}$), the excess $H^+$ ions in the solution cause protonation of the adsorbent surface [62]. On the other hand, at high pH levels ($pH > pH_{ZPC}$), the abundance of OH ions in the solution imparts a negative charge to the adsorbent surface [39]. Therefore, as pH decreases, the KP surface gets protonated, thereby repelling the cationic dye CV molecules, preventing dye molecules from adhering to the surface. While on increasing the pH, a negative charged occur on the surface of activated KP, which favors the binding of cationic dye due to electrostatic attraction, resulting in enhanced adsorption [20].

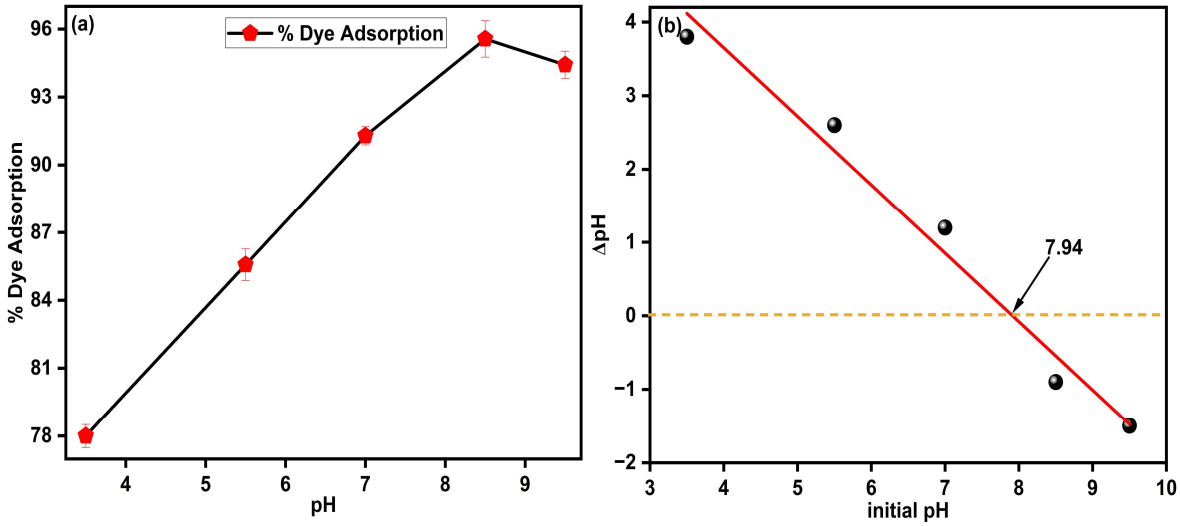


**Figure 8.** Plots of (a) Impact of pH variation and (b) point zero charge ($pH_{ZC}$) on the adsorbent

### 4.2.5 Isotherms

Figure 9 shows isotherm plots for the CV uptake on the bio-sorbent activated KP, and computed values are presented in Table 1. Experimental data for the uptake of CV using Activated KP were found to best fit with the Langmuir model, with $R_2$ = 0.99 for CV, suggesting homogeneous monolayer adsorption on the adsorbent surface. The $R_L$ was calculated to be 0.35. The $q_{max}$ represents the maximum amount of dye adsorbed per unit weight of adsorbent to form a complete monolayer on the surface (mg/g), dye sorption capacities ($q_{max}$)

were calculated based on the Langmuir isotherm model. Hence, the $q_{max}$ of the adsorbent was calculated using the Langmuir isotherm, and it was found to be 33.33 mg/g for CV (20 mg/L).

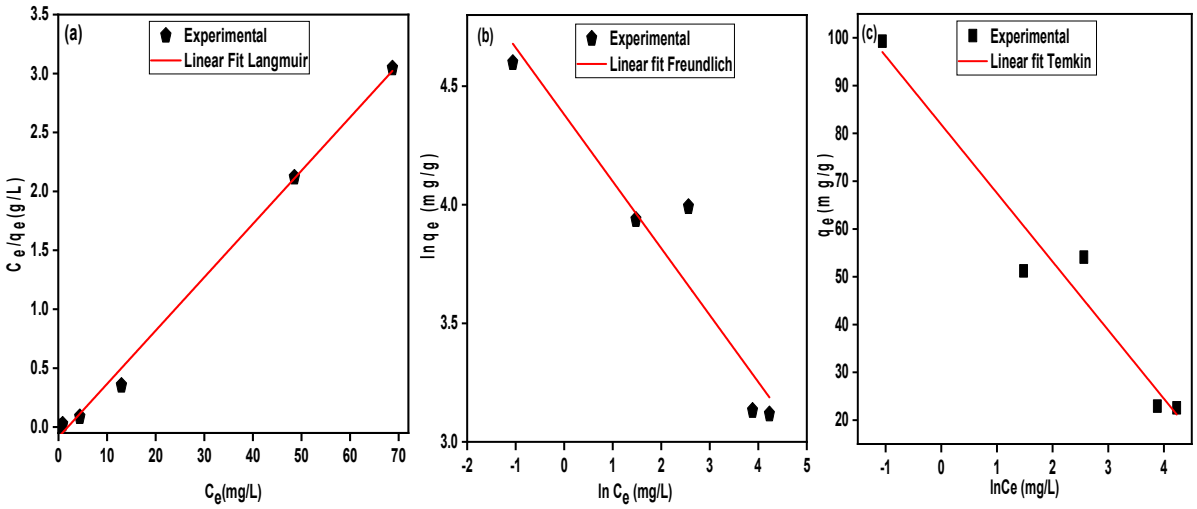


**Figure 9.** Isotherm plots for (a) Langmuir, (b) Freundlich, (c) Temkin Model.

**Table 1.** Calculated Parameters using Various Models.

| **Models** | **Slope & Intercept** | **Parameters** | **Parameter value** |
|---|---|---|---|
| **Langmuir** | Slope = 0.03<br>Intercept =0.085 | $R^2$ | 0.99 |
| | | $q_m$ (mg $g^{-1}$) | 33.33 |
| | | $K_L$ (L $mg^{-1}$) | 0.35 |
| **Freundlich** | Slope = 0.282<br>Intercept = 4.38 | $R^2$ | 0.90 |
| | | $K_F$ (mg $g^{-1}$) (L mg)$^{1/n_f}$ | 79.83 |
| | | $n_f$ | 3.54 |
| **Temkin** | Slope = 14.34<br>Intercept = 81 | $R^2$ | 0.9 |
| | | $A_T$ (L $g^{-1}$) | 2.81 |

### 4.2.6 Kinetics

In order to elucidate the adsorption mechanism, the experimental data were fitted with various kinetic models. The linear fitting of the data using each model is illustrated in Figure 10, and the associated kinetic parameters are summarized in Table 2.

The experimental data exhibited excellent correlation with the pseudo-second-order kinetic model having $R^2 = 0.999$, suggesting that chemisorption governs the rate-determining step of the process. The initial adsorption rate (h) for CV was found to be 18.71 mg/g/min. Thus, the adsorption of CV on activated KP may comprises in three steps: (i) initial physical sorption, (ii) chemical sorption, and (iii) possible saturation at the equilibrium stage.

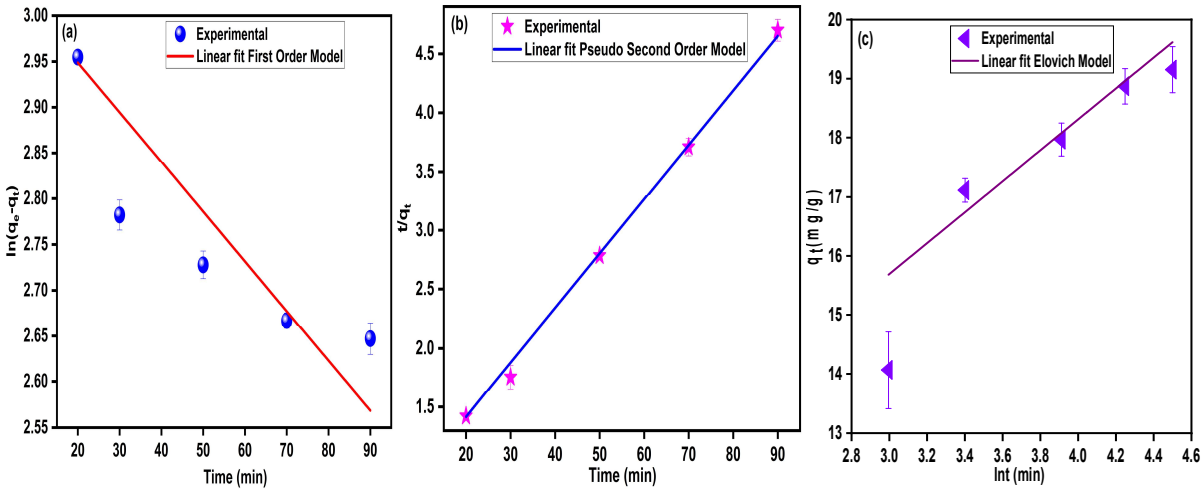


**Figure 10.** Plots of kinetics (a) parameters using Various Models.

**Table 2.** Calculated Parameter for Kinetic Models.

| Kinetics Models Plots | Slope | Intercept | Parameters | Values of Parameters |
|---|---|---|---|---|
| **First order:** $\ln(q_e - q_t) = \ln q_e - K_1 t$ $K_1$ is rate constant | -0.005 | 3.057 | $R^2$ | 0.859 |
| | | | $K_1$ (min $^{-1}$) | 0.005 |
| | | | $q_e$ (mg g$^{-1}$) | 21.26 |
| **Pseudo-second order:** $\frac{t}{q_t} = \frac{1}{k_2 q_e^2} + \frac{t}{q_e}$ $k_2$ is the rate constant $h = k_2 q_e^2$ ; h is the initial adsorption rate | 0.0462 | 0.492 | $R^2$ | 0.999 |
| | | | $K_2$ (g mg$^{-1}$ min$^{-1}$) | 0.004 |
| | | | $q_e$ (mg g$^{-1}$) | 21.64 |
| | | | h (mg g$^{-1}$ min$^{-1}$) | 18.71 |

| | | | | |
|---|---|---|---|---|
| **Elovich model:** $q_t = \beta \ln(\alpha\beta t)$, β is the desorption constant, if α > β, implies chemical sorption | 2.61 | 7.84 | $R^2$ | 0.78 |
| | | | α (mg $g^{-1}$ $min^{-1}$) | 7.23 |
| | | | β (g $mg^{-1}$) | 0.383 |

### 4.2.7 Impact of Temperature

Temperature is a critical parameter influencing the adsorption efficiency of dyes onto adsorbents. The adsorption of crystal violet (CV) dye onto alkali-activated AKP was examined at different temperatures, varied with a temperature interval of 10°C, while maintaining all other experimental conditions identical to those used in the contact time study. The thermodynamic parameters, such as enthalpy, entropy, and Gibbs' free energy, were evaluated using equations:

$$k_e = \frac{q_e}{C_e} \qquad (11)$$

$$\Delta G^0 = -RT \ln K_e \qquad (12)$$

$$\ln K_e = \frac{\Delta S^0}{R} - \frac{\Delta H^0}{RT} \qquad (13)$$

$K_e$ represents the equilibrium constant, qe presents the adsorption capacity (mg/g), Ce is the concentration of the dye at equilibrium, R is the gas constant (8.314 J/K mol), and T represents the temperature in Kelvin (K).

The computed thermodynamic parameters are summarized in Table 3, and Figure 11 illustrates the ln K versus 1/T plot and the effect of temperature on adsorption capacity. It was observed that, the rate of adsorption increases with rise in temperature, resulting in a higher dye adsorption efficiency. It is attributed to the increasing entropy of adsorbate molecules and their corresponding increase in kinetic energy, which facilitates diffusion and interaction with the adsorbent's active sites. Furthermore, elevated temperatures increase molecular mobility, resulting in more frequent and effective collisions between CV dye molecules and the surface

of the activated KP. The positive correlation between temperature and adsorption efficiency confirms that the adsorption process is endothermic in nature [59].

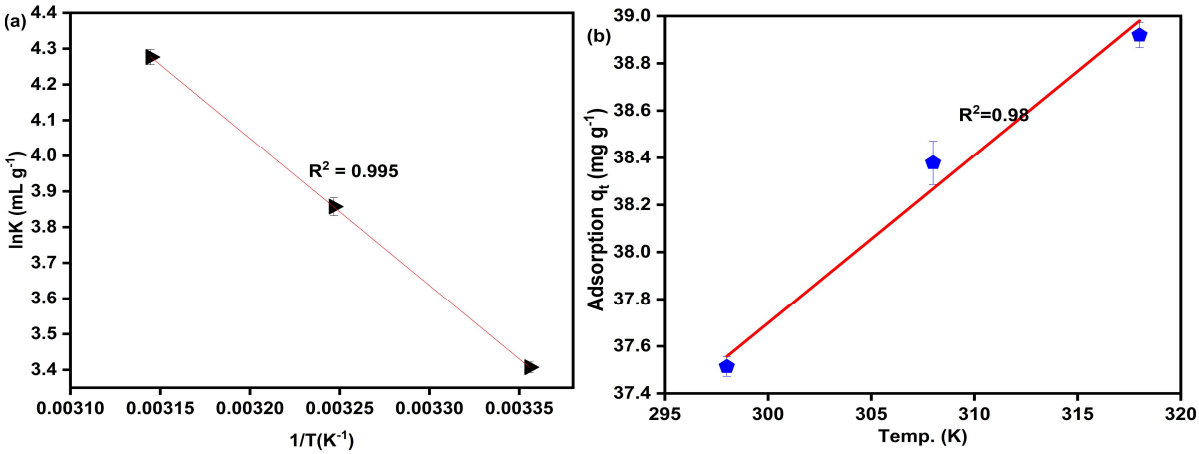


**Figure 11.** Plots for (a) ln K versus 1/T for CV and (b) influence of temperature on adsorption capacity for CV.

**Table 3.** Temperature-dependent parameters for CV uptake

| Temperature (K) | Δ H (KJ mol$^{-1}$) | Δ S$^o$ (J mol$^{-1}$K$^{-1}$) | Δ G$^o$ (KJ mol$^{-1}$) |
|---|---|---|---|
| 298.15 | 34.267 | 143.25 | -8.423 |
| 308.15 | | | -9.538 |
| 318.15 | | | -10.579 |

## 4.3 Binary mixture of Dye

To evaluate the applicability of the synthesized adsorbent in more complex systems, a binary dye adsorption study was conducted using crystal violet (CV) and methylene blue (MB). Equal concentrations of both dyes (20 mg/L each) were mixed in a 1:1 ratio, and 0.15 g of alkali-activated *Kalanchoe Pinnata* (KP) was added to it. The mixture was agitated under dark conditions at 100 rpm for 90 min under ambient temperature to ensure equilibrium adsorption. The absorption maxima for CV and MB were recorded at 589 nm and 662 nm, respectively. As shown in Figure 12a, Activated KP demonstrated notable adsorption efficiencies of 91% for CV and 82% for MB in the binary system. The slightly lower removal efficiency compared

to single-dye systems may be attributed to the competitive adsorption behavior between the two dyes for the limited number of active sites on the adsorbent surface. These results indicate that activated KP possesses substantial adsorption efficiency under multi-dye conditions, highlighting its applicability in real-time wastewater treatment scenarios.

## 4.4 Regeneration and Recyclability

To evaluate the reusability of the synthesized biosorbent, regeneration studies were performed. To perform this, the used biosorbent was collected and washed sequentially with 0.5 M NaOH and ethanol solutions. It helps to desorb the retained dye molecules and regenerate the active binding sites. The regenerated material was then rinsed with distilled water to remove residual NaOH and ethanol, followed by drying at ambient temperature. Then the dried biosorbent was reused for the next adsorption cycles. This process was repeated upto 4 regeneration cycles as depicted in Figure 12b. The biosorbent maintained a dye removal efficiency above % even after 4 consecutive cycles, indicating excellent structural stability and regeneration capability. There is a slight decrease in adsorption efficiency observed after repeated use, which may be attributed to the partial blockage or loss of some active sites during successive regeneration steps. Nevertheless, the high retention of adsorption performance confirms the material's strong potential for sustainable and cost-effective wastewater treatment applications. Therefore, it can be concluded that the alkali-activated KP biosorbent can be effectively regenerated and reused multiple times without significant loss of activity, making it feasible for large-scale environmental remediation.

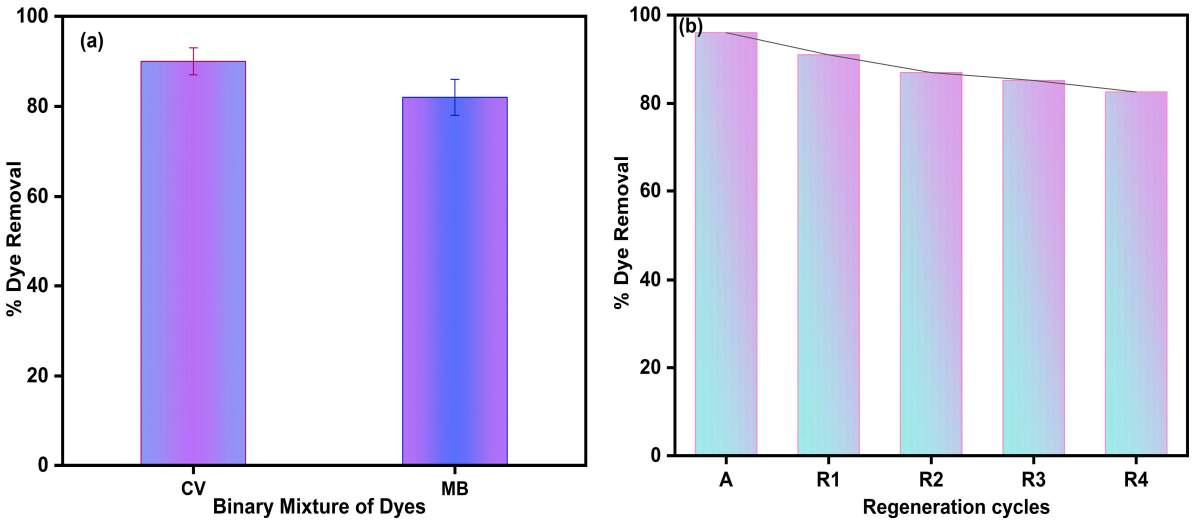


**Figure 12.** Plots for (a) binary mixture of CV and MB, (b*)* regeneration cycles of biosorbent for removal of CV.

## 4.5 Adsorption in Real Wastewater Samples

The dye removal efficiency of the adsorbent was assessed in real waste water samples. The sample was collected from the Industrial Area, Badli, New Delhi. The dye concentration has been spiked in a sample having dyes, metals, and other effluents. Thus, in order to check the effect of model dye (CV), dyes of known concentration was added to the sample and the adsorption efficiency was compared with distilled water. It was observed that the percentage removal efficacy of dye in real sample was found to be 83.36 %, shown in Figure 12c.

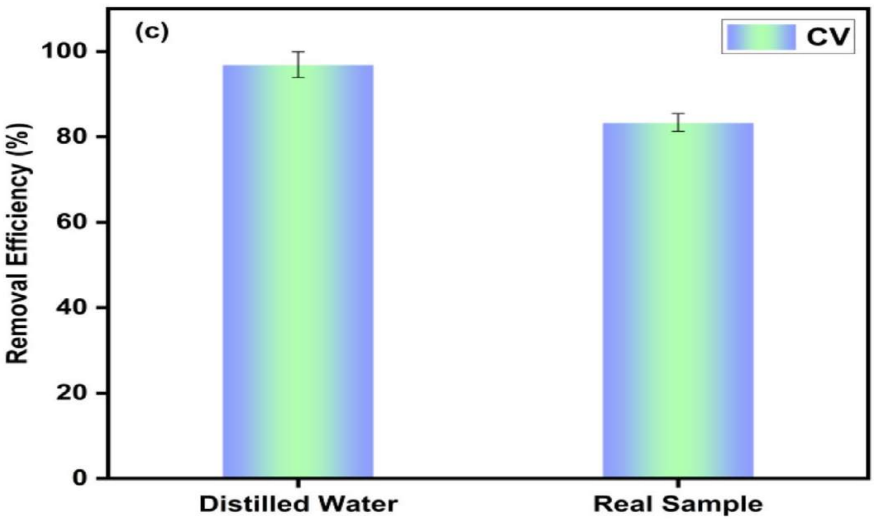


**Figure 12.** Plot for (c) Removal efficiency in real wastewater sample

## 4.6 Probable Mechanism

It is an important fact to note that the surface charge can modulate the dye adsorption. Accordingly, the present adsorption is associated with electrostatic attraction, weak van der Waals forces, and π-π stacking, as presented in Figure 13. The π-π stacking presents between the aromatic rings of dye and the phenolic group present in the structures of sorbent. This interaction allows adsorption on surface of adsorbent. While weak van der Waals interactions between the dye molecules and the biosorbent surface which contributes to the overall affinity of dye to the sorbent. Adsorption is higher above $pH_{zpc}$ due to steric repulsion between the cationic dye and the negative surface of the adsorbent [52], [63]. This explanation may be supported by the DLS study, which shows that a negative charge on the adsorbent facilitates the adsorption of the CV dye on the sorbent surface.

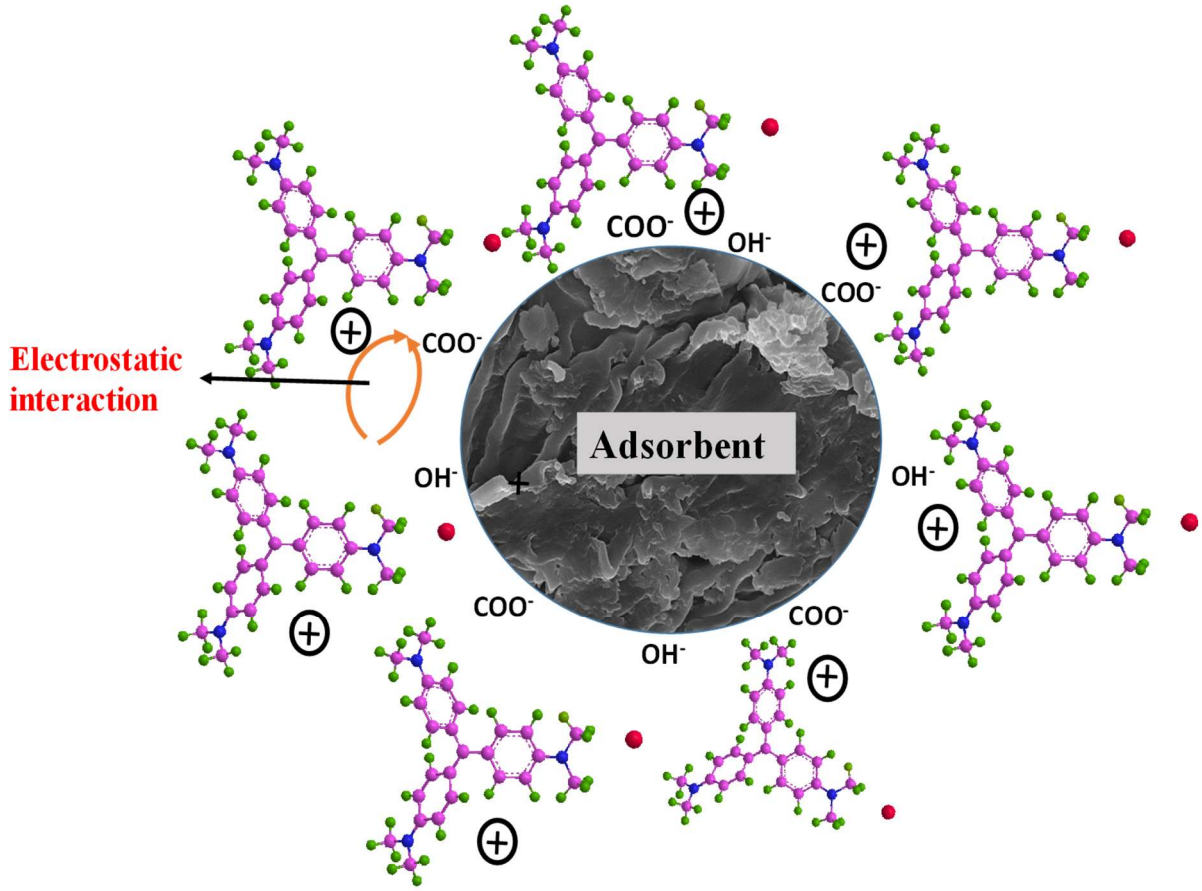


**Figure 13.** Mechanism of adsorption on the adsorbent.

## 4.7 Different Biosorbent

The present study was also compared with the initial dye concentration, removal efficiency and adsorption capacity of the synthesized adsorbent with some reported sorbents presented in Table 7. It was observed that our synthesized sorbent has better adsorption capacity, better removal percentage, and adsorption capacity compared with the reported adsorbents.

**Table 4.** Different Adsorbents reported for the sequestration of dyes

| | Adsorbent | Adsorbent dosage (g) | % Removal | Adsorption capacity (mg/g) | Ref. |
|---|---|---|---|---|---|
| 1 | Guinea grass (Megathyrsus maximus) | 0.250g | 95 | 21.44 (RB), 7.94(MB) | [64] |
| 2 | Teak Sawdust | — | 94 | 1.35 | [65] |
| 3 | Cashew shell | 0.2g | 98.5 | 5.18 | [66] |
| 4 | GG/PAM | — | 90 | 31 | [67] |
| 5 | Sawdust | 0.2g | 98 | 9 | [68] |
| 6 | ZnO activated wood sawdust | 1.2g | 94 | 35 | [69] |
| 7 | Activated *Kalanchoe Pinnata* | 0.015g | 96 | 33.33 | Present Study |

# Chapter 5
# CONCLUSION

In this study, dried KP leaves are utilized as a biowaste that serves as a biosorbent for the sequestration of CV dye from aqueous media. The sorbent morphology was characterized using FESEM and shows a fragmented and porous surface, which supports the adsorption phenomenon. Similarly, active surface area was also calculated and was found to be higher (12.097 $m^2/g$) in the case of activated KP, while lower (5.719 $m^2/g$) in KP, suggesting that activated KP is favorable for the adsorption. The impact of various parameters, including contact time, concentrations, and others, was studied, and it was found that ~96% removal of CV dye from aqueous media in 90 min. The maximum adsorption capacity was found to be 33.33 mg/g. Further, isotherm and kinetic studies were performed, which revealed that sorbent follows monolayer adsorption and pseudo-second-order ($R^2$ = 0.99). In addition to that, regeneration studies were also performed, and it was found that the sorbent efficiently adsorbs CV dye after 4 cycles. The structural analysis of the sorbent was conducted after adsorption also, reveals that structure was intact after adsorption. Thereby, it concludes that the synthesized biowaste based sorbent can be serves as a good candidate for practical importance in real scale field.

## REFERENCES:

[1] "S. Mallakpour, F. Tabesh, Green and plant-based adsorbent from tragacanth gum and carboxyl-functionalized carbon nanotube hydrogel bionanocomposite for the super removal of methylene blue dye, Int. J. Biol. Macromol. 166 (2021) 722–729. https://doi.org/10.1016/j.ijbiomac.2020.10.229".

[2] "A. Plessis, Commentary Persistent degradation : Global water quality challenges and required actions, One Earth 5 (2022) 129–131. https://doi.org/10.1016/j.oneear.2022.01.005.".

[3] "F. Abbasi, M.T. Yaraki, A. Farrokhnia, M. Bamdad, Keratin nanoparticles obtained from human hair for removal of crystal violet from aqueous solution: Optimized by Taguchi method, Int. J. Biol. Macromol. (2019). https://doi.org/10.1016/j.ijbiomac.2019.12.065.".

[4] "M. Zubair, N. Dalhat, N. Jarrah, N.I. Blaisi, Adsorption Behavior and Mechanism of Methylene Blue , Crystal Violet , Eriochrome Black T , and Methyl Orange Dyes onto Biochar-Derived Date Palm Fronds Waste Produced at Different Pyrolysis Conditions, Chem. Rev. 120 (2020) 8378–8415.".

[5] "Y.Z. Xueli Baia, Zhaoyang Bai, Dandan Xue, Huiyan Sun, Xin Huanga, Yongxiang Zhao, OXIDATION OF CYCLOHEXANOL ON PHOSPHOTUNGSTIC ACID ANION INTERCALATED LAYERED DOUBLE HYDROXIDES WITH AQUEOUS H2 O2 AS OXIDANT, Quim. Nova 41 (2018) 5–9.".

[6] "A. El-Baz, I. Hendy, A. Dohdoh, M. Srour, Adsorption technique for pollutants removal; current new trends and future challenges – A Review, Egypt. Int. J. Eng. Sci. Technol. 32 (2020) 1–24. https://doi.org/10.21608/eijest.2020.45536.1015.".

[7] "A.W. Carpenter, C.F. De Lannoy, M.R. Wiesner, Cellulose nanomaterials in water treatment technologies, Environ. Sci. Technol. 49 (2015) 5277–5287. https://doi.org/10.1021/es506351r".

[8] "P. Yadav, S.G. Warkar, A. Kumar, Development of graphene oxide-incorporated biopolymer-carboxymethyl tamarind kernel gum-based hydrogel as an effective adsorbent for the sequestration of dye pollutants, Polym. Eng. Sci. 64 (2024) 1–18. https://doi.org/10.1002/pen.26883.".

[9] "M. Bilal, I. Ihsanullah, M. Younas, M. Ul, H. Shah, Recent advances in applications of low-cost adsorbents for the removal of heavy metals from water : A critical review, Sep. Purif. Technol. 278 (2022) 119510. https://doi.org/10.1016/j.seppur.2021.119510.".

[10] "Y. Oladosu, M.Y. Rafii, F. Arolu, S.C. Chukwu, M.A. Salisu, I.K. Fagbohun, T.K. Muftaudeen, S. Swaray, B.S. Haliru, Superabsorbent Polymer Hydrogels for

Sustainable Agriculture: A Review, Horticulturae 8 (2022) 1–17. https://doi.org/10.3390/horticulturae8070605".

[11] " P. Yadav, Rachana, V. Jha, Divyanshu, S.G. Warkar, A. Kumar, Harnessing alkali assisted Calotropis gigantea leaf as phytosorbent for removal of crystal violet from water, Int. J. Phytoremediation (2025). https://doi.org/10.1080/15226514.2025.2533522.".

[12] "P. Yadav, K. Kashyap, S.G. Warkar, A. Kumar, FeO NPs-Loaded Guar Gum / Xanthan Gum-Based Hydrogel : A Sustainable Approach for Cationic Dye Removal, ChemistrySelect 10 (2025) 1–16. https://doi.org/10.1002/slct.202500293.".

[13] "A. Kafle, A. Timilsina, A. Gautam, K. Adhikari, A. Bhattarai, Phytoremediation : Mechanisms , plant selection and enhancement by natural and synthetic agents, Environ. Adv. 8 (2022) 100203. https://doi.org/10.1016/j.envadv.2022.100203.".

[14] "E. Vialkova, E. Korshikova, A. Fugaeva, Phytosorbents in Wastewater Treatment Technologies : Review, Water 16 (2024) 2626.".

[15] " J. Mohanta, R. Kumari, M.A. Qaiyum, B. Dey, S. Dey, Alkali assisted hydrophobic reinforcement of coconut fiber for enhanced removal of cationic dyes: equilibrium, kinetics, and thermodynamic insight, Int. J. Phytoremediation 23 (2021) 1423–1431. https://doi.org/10.1080/15226514.2021.1901850.".

[16] "R. Mahato, M.A. Qaiyum, P.P. Samal, S. Dutta, B. Dey, S. Dey, Exploring the promising potential of fallen bamboo leaves ( Bambusa bambos ) for efficient removal of crystal violet from wastewater , Int. J. Phytoremediation 0 (2022) 1–10. https://doi.org/10.1080/15226514.2022.2125498.".

[17] "A. Rout, M.A. Qaiyum, P.P. Samal, S. Dutta, B. Dey, S. Dey, Brinjal (Solanum melongena) stalk waste as an effective scavenger for Eriochrome Black-T from water and wastewater: an approach towards waste to best , Int. J. Phytoremediation 0 (2022) 1–9. https://doi.org/10.1080/15226514.2022.2123445.".

[18] "N. Tahir, H.N. Bhatti, M. Iqbal, S. Noreen, Bio-molecules composite with peanut hull waste and application for Crystal Violet adsorption, Int. J. Biol. Macromol. (2016). https://doi.org/10.1016/j.ijbiomac.2016.10.013.".

[19] P. Yadav, U. Papola, S. G. Warkar, and A. Kumar, "Alkali-Modified Kalanchoe pinnata Leaves as a Biosorbent for Sequestration of Crystal Violet Dye," *ChemistrySelect*, vol. 11, no. 15, Apr. 2026, doi: 10.1002/slct.202507526.

[20] "M.A. Qaiyum, J. Mohanta, R. Kumari, P.P. Samal, B. Dey, S. Dey, Alkali treated water chestnut (Trapa natans L.) shells as a promising phytosorbent for malachite green removal from water, Int. J. Phytoremediation 24 (2022) 822–830. https://doi.org/10.1080/15226514.2021.1977912".

[21] "H. Barik, A. Qaiyum, B. Dey, S. Dey, Integrated activation strategy of mahua seed cake for efficient wastewater treatment : a sustainable approach for methylene blue removal, Biomass Convers. Biorefinery (2024). https://doi.org/10.1007/s13399-024-06040-z.".

[22] "Z.F. Akl, E.G. Zaki, S.M. ElSaeed, Green Hydrogel-Biochar Composite for Enhanced Adsorption of Uranium, ACS Omega 6 (2021) 34193–34205. https://doi.org/10.1021/acsomega.1c01559.".

[23] "S. Das, P.P. Samal, A. Qaiyum, B. Dey, S. Dey, Neolamarckia cadamba ( cadamba ) waste pulp as a natural and techno-economic scavenger for methylene blue from aqueous solutions, Int. J. Phytoremediation 26 (2024) 208–218. https://doi.org/10.1080/15226514.2023.2232861.".

[24] "M. Zhang, B. Gao, S. Varnoosfaderani, A. Hebard, Y. Yao, M. Inyang, Preparation and characterization of a novel magnetic biochar for arsenic removal, Bioresour. Technol. 130 (2013) 457–462. https://doi.org/10.1016/j.biortech.2012.11.132.".

[25] "P.B. Rajsekhar, R.S.A. Bharani, M. Ramachandran, K.J. Angel, S. Priya, V. Rajsekhar, The ' Wonder Plant ' Kalanchoe pinnata ( Linn .) Pers .: A Review, J. Appl. Pharm. Sci. 6 (2016) 151–158. https://doi.org/10.7324/JAPS.2016.60326.".

[26] "M. Khurshid, The miracle plant ( Kalanchoe pinnata ): A phytochemical and pharmacological review, Int. J. Res. Ayurveda Pharm. 2 (2015) 1478–1482.".

[27] "E. Seseña-m, Potential of Kalanchoe pinnata as a Cancer Treatment Adjuvant and an Epigenetic Regulator, Molecules 27 (2022) 1–18.".

[28] "X. Liu, K. Sathishkumar, H. Zhang, K.K. Saxena, F. Zhang, S. Naraginti, K. Anbarasu, R. Rajendiran, Frontiers in environmental cleanup : Recent advances in remediation of emerging pollutants from soil and water, J. Hazard. Mater. Adv. 16 (2024) 100461. https://doi.org/10.1016/j.hazadv.2024.100461".

[29] "M.I. Nkollo, I.O. Efejene, C. Christian, Phytochemistry and pharmacological insights into Kalanchoe pinnata : A brief, J. Med. Res. 2 (2025) 15368110.".

[30] "P. Anastas, N. Eghbali, Green Chemistry : Principles and Practice, Chem. Soc. Rev. 39 (2010) 301–312. https://doi.org/10.1039/b918763b.".

[31] "] S. Jana, J. Ray, B. Mondal, T. Tripathy, Efficient and selective removal of cationic organic dyes from their aqueous solutions by a nanocomposite hydrogel, katira gum-cl-poly(acrylic acid-co-N, N-dimethylacrylamide)@bentonite, Appl. Clay Sci. 173 (2019) 46–64. https://doi.org/10.1016/j.clay.2019.03.009.".

[32] "S. Pandey, N. Son, S. Kim, D. Balakrishnan, M. Kang, Locust Bean gum-based hydrogels embedded magnetic iron oxide nanoparticles nanocomposite: Advanced

materials for environmental and energy applications, Environ. Res. 214 (2022) 114000. https://doi.org/10.1016/j.envres.2022.114000.”.

[33] “J.O. Quansah, T. Hlaing, F.N. Lyonga, P.P. Kyi, S.H. Hong, C.G. Lee, S.J. Park, Nascent rice husk as an adsorbent for removing cationic dyes from textile wastewater, Appl. Sci. 10 (2020). https://doi.org/10.3390/app10103437.”.

[34] “M.G. Ghoniem, F.A.M. Ali, B.Y. Abdulkhair, M.R.A. Elamin, A.M. Alqahtani, S. Rahali, M.A. Ben Aissa, Highly Selective Removal of Cationic Dyes from Wastewater by MgO Nanorods, Nanomaterials 12 (2022) 1–14. https://doi.org/10.3390/nano12061023.”.

[35] “P. Yadav, S.G. Warkar, A. Kumar, Biopolymer-CMTG and m-BPDM Based Hydrogel Composite for Promising Sensing of Zinc, Cadmium, and Mercury in Aqueous Medium, J. Inorg. Organomet. Polym. Mater. 35 (2024) 846–862. https://doi.org/10.1007/s10904-024-03224-y.”.

[36] “H. Barik, M.A. Qaiyum, B. Dey, S. Dey, Integrated activation strategy of mahua seed cake for efficient wastewater treatment: a sustainable approach for methylene blue removal, Biomass Convers. Biorefinery 15 (2025) 11687–11700. https://doi.org/10.1007/s13399-024-06040-z.”.

[37] “H. Barik, M.A. Qaiyum, P.P. Samal, B. Dey, S. Dey, Highly efficient removal of crystal violet dye using citric acid-modified Lotus (Nelumbo nucifera) seed pod, Biomass Convers. Biorefinery 15 (2025) 11835–11849. https://doi.org/10.1007/s13399-024-06027-w.”.

[38] “S. Kalam, S.A. Abu-khamsin, M.S. Kamal, S. Patil, Surfactant Adsorption Isotherms : A Review, (2021). https://doi.org/10.1021/acsomega.1c04661.”.

[39] “G. Issabayeva, S.H. Wong, C.Y. Pang, M.C. Wong, M.K. Aroua, Fluoride removal by low-cost palm shell activated carbon modified with prawn shell chitosan adsorbents, Int. J. Environ. Sci. Technol. 19 (2022) 3731–3740. https://doi.org/10.1007/s13762-021-03448-2.”.

[40] “N. Ayawei, A.N. Ebelegi, D. Wankasi, Modelling and Interpretation of Adsorption Isotherms, J. Chem. 2017 (2017). https://doi.org/10.1155/2017/3039817.”.

[41] “H. Freundlich, Über die Adsorption in Lösungen, Zeitschrift Für Phys. Chemie 57U (1907) 385–470. https://doi.org/10.1515/zpch-1907-5723.”.

[42] “A. Mori, I.L. Maksimov, On the Temkin model of solid-liquid interface, J. Cryst. Growth 200 (1999) 297–304. https://doi.org/10.1016/S0022-0248(98)01397-9.”.

[43] “M. Musah, Y. Azeh, J. Mathew, M. Umar, Z. Abdulhamid, A. Muhammad, Adsorption Kinetics and Isotherm Models: A Review, Caliphate J. Sci. Technol. 4 (2022) 20–26. https://doi.org/10.4314/cajost.v4i1.3.”.

[44] “V. Srihari, A. Das, The kinetic and thermodynamic studies of phenol-sorption onto three agro-based carbons, Desalination 225 (2008) 220–234. https://doi.org/10.1016/j.desal.2007.07.008.”.

[45] “J.C. Bullen, S. Saleesongsom, K. Gallagher, D.J. Weiss, A Revised Pseudo-Second-Order Kinetic Model for Adsorption, Sensitive to Changes in Adsorbate and Adsorbent Concentrations, Langmuir 37 (2021) 3189–3201. https://doi.org/10.1021/acs.langmuir.1c00142.”.

[46] “F. Wu, R. Tseng, R. Juang, Characteristics of Elovich equation used for the analysis of adsorption kinetics in dye-chitosan systems, 150 (2009) 366–373. https://doi.org/10.1016/j.cej.2009.01.014.”.

[47] “A. Bora, N. Karak, Starch and itaconic acid-based superabsorbent hydrogels for agricultural application, Eur. Polym. J. 176 (2022) 111430. https://doi.org/10.1016/j.eurpolymj.2022.111430.”.

[48] “N.A. Yahya, R. Abdul Wahab, N. Attan, M. Abdul Hamid, N. Mohamed Noor, R. Kobun, Ananas comosus Peels Extract as a New Natural Cosmetic Ingredient: Oil-in-Water (O/W) Topical Nano Cream Stability and Safety Evaluation, Evidence-Based Complement. Altern. Med. 2022 (2022). https://doi.org/10.1155/2022/2915644.”.

[49] “Z. Sun, L. Wang, X. Jiang, L. Bai, W. Wang, H. Chen, L. Yang, H. Yang, D. Wei, Self-healing, sensitive and antifreezing biomass nanocomposite hydrogels based on hydroxypropyl guar gum and application in flexible sensors, Int. J. Biol. Macromol. 155 (2020) 1569–1577. https://doi.org/10.1016/j.ijbiomac.2019.11.134.”.

[50] “J. Swain, P. Priyadarsini, S. Atif, Q. Banashree, D. Soumen, Biosorption of Crystal Violet , a Cationic Dye onto Alkali Treated Rauvolfia tetraphylla Leaf : Kinetics , Isotherm and Thermodynamics, Water Conserv. Sci. Eng. (2024). https://doi.org/10.1007/s41101-023-00233-9.”.

[51] “R. Kaur, H. Kaur, Calotropis procera an effective adsorbent for removal of Congo red dye: isotherm and kinetics modelling, Model. Earth Syst. Environ. 3 (2017) 1–13. https://doi.org/10.1007/s40808-017-0274-3”.

[52] “S. Dey, R. Chakraborty, J. Mohanta, B. Dey, Tricosanthes cucumerina: a potential biomass for efficient removal of methylene blue from water, Bioremediat. J. 0 (2022) 1–15. https://doi.org/10.1080/10889868.2022.2086530.”.

[53] “ acrylic acid ) hydrogels obtained by electron beam crosslinking, J. Environ. Chem. Eng. 18 (2022) 1–17. https://doi.org/10.1016/j.chemosphere.2022.134917.”.

[54] “M.A. Lillo-Ródenas, D. Cazorla-Amorós, A. Linares-Solano, Understanding chemical reactions between carbons and NaOH and KOH: An insight into the chemical

activation mechanism, Carbon N. Y. 41 (2003) 267–275. https://doi.org/10.1016/S0008-6223(02)00279-8.”.

[55] “M. Kadhom, N. Albayati, H. Alalwan, M. Al-Furaiji, Removal of dyes by agricultural waste, Sustain. Chem. Pharm. 16 (2020) 100259. https://doi.org/10.1016/j.scp.2020.100259.”.

[56] “S. Parida, P.P. Samal, B. Dey, S. Dey, Wodyetia bifurcata (foxtail palm tree) leaves as a super-augmented instantaneous methylene blue remover from simulated water and wastewater, Environ. Monit. Assess. 196 (2024) 848. https://doi.org/10.1007/s10661-024-13033-y.”.

[57] “R. Kumari, A. Sircar, S. Dey, M. Qaiyum, N. Bist, Sequestration of a food dye ( sunset yellow ) from wastewater using natural adsorbent : a kinetic , isotherm and interference study, Int. J. Phytoremediation 26 (2024) 1716–1727. https://doi.org/10.1080/15226514.2024.2349964.”.

[58] “J. Pathak, P. Singh, Adsorptive Removal of Congo Red Using Organically Modified Zinc–Copper–Nickel Ternary Metal Hydroxide: Kinetics, Isotherms and Adsorption Studies, J. Polym. Environ. 31 (2023) 327–344. https://doi.org/10.1007/s10924-022-02612-0.”.

[59] “B. Pandey, P. Singh, Statistical Optimization of Process Parameters for Ultrafast Uptake of Anionic Azo Dyes by Efficient Sorbent: Zn/Cu Layered Double Hydroxide, Appl. Organomet. Chem. (2023) 1–18. https://doi.org/10.1002/aoc.7072.”.

[60] “I. Rani, S.G. Warkar, A. Kumar, Removal of Cationic Crystal Violet dye using Zeolite-Embedded Carboxymethyl Tamarind Kernel Gum (CMTKG) based Hydrogel Adsorbents, ChemistrySelect 8 (2023). https://doi.org/10.1002/slct.202301434.”.

[61] “P. Yadav, Rachana, V. Jha, Divyanshu, S.G. Warkar, A. Kumar, Harnessing alkali assisted Calotropis gigantea leaf as phytosorbent for removal of crystal violet from water, Int. J. Phytoremediation 0 (2025) 1–15. https://doi.org/10.1080/15226514.2025.2533522.”.

[62] “K.G. Akpomie, J. Conradie, Efficient adsorptive removal of paracetamol and thiazolyl blue from polluted water onto biosynthesized copper oxide nanoparticles, Sci. Rep. 13 (2023) 1–16. https://doi.org/10.1038/s41598-023-28122-0.”.

[63] “A. Bashir, B. Saleh, Powdered Beet Red Roots Using as Adsorbent to Removal of Methylene Blue Dye from Aqueous Solutions, Waset 22-23 (2015).”.

[64] “M. A. O. Y. Weeratunge, M. D. N. Dinusha, R. M. M. K. Karunathilaka, and N. Priyantha, ‘Comparative Adsorption Characteristics of Methy- lene Blue on Raw Leaves and Biochar of Guinea Grass (Megathyrsus maximus),’ Discover Chemistry 3 (2026): 1–20.”.

[65] “T. W. Sawdust, T. Training, N. Tenggara, N. Sciences, T. Training, and E. N. Tenggara, ‘Adsorption of Methylene Blue Using the Biosorbent of Teak Sawdust, Orbital Electron,’ Journal of Chemistry 17 (2025): 415–425.”.

[66] “ R. Sharma, S. Kalia, B. S. Kaith, and M. K. Srivastava, ‘Synthe- sis of Guar Gum-Acrylic Acid Graft Copolymers Based Biodegradable Adsorbents for Cationic Dye Removal,’ International Journal of Plastics Technology 20 (2016): 294–314, https://doi.org/10.1007/s12588- 016- 9156- 1. ”.

[67] “ J. N. Hiremath and B. Vishalakshi, ‘Evaluation of a pH-responsive Guar Gum-Based Hydrogel as Adsorbent for Cationic Dyes: Kinetic and Modelling Study,’ Polymer Bulletin 72 (2015): 3063–3081, https://doi.org/ 10.1007/s00289- 015- 1453- x. ”.

[68] “C. Bouyahia, M. Rahmani, M. Bensemlali, et al., ‘Influence of Extraction Techniques on the Adsorption Capacity of Methylene Blue on Sawdust : Optimization by Full Factorial Design,’ Materials Science for Energy Technologies 6 (2023): 114–123, https://doi.org/10.1016/j.mset.2022. 12.004 . ”.

[69] “N. S. M. Sayed, A. S. A. Ahmed, M. H. Abdallah, and G. A. Gouda, ‘ZnO@ Activated Carbon Derived From Wood Sawdust as Adsorbent for Removal of Methyl Red and Methyl Orange From Aqueous Solutions,’ Scientific Reports 14 (2024): 5384.”.